Generality of the Branched Pathway in Transcription Initiation by *E.coli* RNA Polymerase

Motoki Susa
Doctor of Philosophy

Department of Genetics
School of Life Science
The Graduate University for Advanced Studies

2001

Table of Contents

Abstract

Transcription initiation has long been assumed to be a sequence composed of four steps: binding of RNA polymerase to a promoter, isomerization of the resulting binary complex accompanied by strand opening, iterative synthesis and release of abortive transcripts, and escape of the enzyme from the promoter. These steps are either chemical step essential to synthesize long RNA or explain a phenomenon that is observed for all RNA polymerases examined. Although additional steps could exist, the sequence has been considered as the complete mechanism, mainly because of the lack of evidence for further complications. In fact, the sequential pathway explained the results previously obtained in particular for the initiation at the T7A1 promoter.

However, the existence of branched reaction pathway was recently discovered in the initiation at the λP_RAL, *lac*UV5 and *malT* promoters, where a part of the enzyme-promoter complex is arrested at the promoter. This finding raises a new question which mechanism is more general and which is an exceptional case. From kinetic viewpoint, the sequential pathway is a special case of the branched pathway proposed. In a test of the generality of the pathway, one of the key criteria is whether or not initiation at the T7A1 promoter actually follows the branched pathway. I addressed this question by using several kinetic and biochemical techniques.

In the most sensitive kinetic assay, moribund complex, which synthesize only abortive transcripts as branched reaction, was detected and its amount increased in a low salt condition. In the gel mobility-shift assay and DNA footprinting with exonuclease III, a small amount of the complex arrested at the promoter was detected and its level was significantly raised in the low salt condition. The results of the DNA footprinting as well as that by Fe^{2+} cheleted at the active site of the enzyme demonstrated the existence of a fraction of binary complex that dislocates from its position of productive subspecies, suggesting that moribund subspecies is forward tracked compared with productive subspecies. This also suggests the existence of a branching point in the stage of binary complex that has been proposed for the initiation at the λP_RAL. These results prove that the initiation at the T7A1 promoter also follows the common branched pathway.

The amount of arrested complex formed at the T7A1 promoter is less than 3% of that of binary complex that initially exist before adding NTPs. This explains the reason why the behaviors of the initiation at the promoter apparently follow the sequential pathway. The small fraction could be due to the rapid conversion between moribund and productive subspecies. The rapid conversion was confirmed by measuring the rates of their dissociation and the rates

were 7 times faster than those for the λP_RAL promoter. In conclusion, the branched pathway is more general mechanism and the case of T7A1 promoter is a particular one due to the rapid conversion.

I next addressed the question whether or not the branched pathway has physiological significance in *E. coli* cell. The clue is the effect of the transcription factors GreA and GreB on promoter arrest, which was previously shown to relieve the arrest in the initiation at the λP_RAL promoter by introducing reversibility in the conversion of moribund subspecies into productive one.

An *E.coli* strain with disrupted *greA* and *greB* grows well in LB medium at 37 ℃, but does not grow at 25 ℃. It was also sensitive to Mn^{2+} or Zn^{2+}-in LB medium. By using *E.coli* gene array, the candidate genes whose expressions are changed in the strain with disrupted *greA* and *greB* was previously selected. By using Northerm blotting, I confirmed that mRNA levels of at least 3 genes, *cspA*, *rpsA* and *atpC*, are decreased by the disruption of *greA* and *greB*. Full-length transcription from their promoters was observed to be enhanced in the presence of GreA or GreB in a purified reconstitution system. The addition of the factors reduced abortive transcripts, suggesting that the factors increased the yield of full-length transcript by mitigating the promoter arrest. Among the promoters tested, *atp* promoter, the major promoter of *atp* operon, was examined most detail. Primer extension analysis confirmed that the transcript transcribed from the *atp* promoter was indeed reduced by the disruption of *greA* and *greB*. The formation of moribund complex at the *atp* promoter was confirmed by the most sensitive kinetic assay. In conclusion, the branched pathway is working not only in vitro but also in *E.coli*, and the GreA and GreB regulate transcription of various genes by the mechanism. This finding also claims that the Gre factors are bonafide initiation factors, although they were discovered as elongation factors that mitigate elongation arrest in vitro.

Introduction

Transcription in prokaryote is carried out by a multi-subunit enzyme, DNA-dependent RNA polymerase which contains five subunits with the stoichiometry $\alpha_2\beta\beta'\sigma$. The σ subunit is bound relatively weak to the rest of the enzyme (the core enzyme) and is responsible for binding to a specific segment of DNA, called promoter, that signals where RNA synthesis should begin (1). The start of transcription by the RNA polymerase involves several biochemical steps; i) RNA polymerase binds to a promoter, and the resultant complex is called closed binary complex. ii) DNA helix is partially unwound in the binary complex to expose a short stretch of single-stranded DNA that acts as a template for an incoming ribonucleotide (NTP) with base-pairing. This change is accompanied by unknown changes in conformation of the DNA-polymerase complex and called isomerization. The resultant complex is called open binary complex. iii) Short transcripts are iteratively synthesized and released. This step is called abortive synthesis, and ternary complex, composed of the DNA, RNA and RNA polymerase, is formed in this step. iv) The enzyme escapes from the promoter accompanied by establishment of continuous elongation. This step is called promoter escape or promoter clearance. Transcription initiation is defined so as to include these steps.

Although these four steps in this order are essential to initiate transcription of long transcripts (1), this sequence does not necessarily represent the complete mechanism of transcription initiation, since additional step(s) could exist. Nevertheless, it has long been assumed that the sequence is the complete mechanism, mainly because of the lack of evidence for further complications. This simplest mechanism is called the sequential pathway model (Scheme 1A). Among kinetic studies of transcription initiation from various promoters, those involving the bacteriophage T7A1 promoter in particular show two distinct behaviors that are characteristic of the sequential model. Firstly, the binary complex synthesizes a stoichiometric amount of full-length transcript in a single-round transcription (2). Secondly, abortive synthesis does not occur after the synthesis of full-length transcript (3), consistent with the view that the transcription complex engaged in abortive synthesis is a precursor of the elongation complex synthesizing a long RNA. However, these results do not prove that the sequential pathway is applicable to initiation at all promoters, nor even at the T7A1 promoter in all conditions.

On the other hand, the above behaviors are not observed in single-round transcription from λP_RAL and *lac*UV5 promoters. The synthesis of full-length transcript initiated at these promoters was completed within 5 min, but abortive transcripts were continuously synthesized for at least 20 min (4). Furthermore, The amount of full-length transcript from these promoters is significantly less than stoichiometric with that of the binary complex (5). These indicate the

presence of a transcription complex that are capable only of abortive synthesis, and not of productive elongation. This non-productive complex is termed "Moribund complex" and becomes slowly inactive at the promoter. These discrepancies are not attributable to heterogeneity in the preparation of RNA polymerase used, for the following reasons. RNA polymerase that has been re-isolated from the run-off elongation complex displays the same persistent synthesis of abortive transcripts at the λP_RAL promoter as the original enzyme, indicating that a fraction of the productive enzyme becomes non-productive (4). The amount of full-length product in single-round transcription from the λP_RAL promoter is much less than that of the binary complex because of the existence of the non-productive complexes. This fraction almost disappears when a transcription factor GreA (or GreB) and a high concentration of the initiation nucleotide are present, indicating that the non-productive enzyme can be converted into productive (6). Therefore, two fractions of RNA polymerase-promoter complex that produces or does not produce full-length product are originated from a homogeneous preparation of the enzyme, implying the existence of non-productive pathway(s) that cause(s) the persistent abortive synthesis. In other words, the initiation pathway is branched at some stage before abortive synthesis at the promoters.

From the observations above, a model for initiation from the λP_RAL promoter has suggested as shown in Scheme 1B. There is a branching point before abortive synthesis, at the stage of binary complex. The moribund complex is first generated in the non-productive branch of initiation, the promoter-arrested pathway. In this transcription unit, the moribund complex is slowly converted into inactive dead-end complex (4, 7). The moribund complex is also identifiable in initiation at the *malT* promoter (8), suggesting that the branched pathway may be applicable to initiation at many promoters.

In a test of the generality of the branched pathway model, one of the key criteria would be whether or not initiation at the T7A1 promoter, whose mechanism appears the most sequential, actually follows the branched pathway. From kinetic viewpoint, a branched pathway could appear to be sequential under appropriate conditions. If the moribund complex converted into a productive complex before converting into a dead-end complex, most transcription complexes would finally indulge in productive elongation and the branched pathway would become effectively equivalent to the sequential. In this case, a stoichiometric amount of the full-length transcript would be synthesized in single-round transcription and abortive transcripts would not be produced after completion of the full-length synthesis. Indeed, this situation occurs at the λP_RAL promoter in the presence of the Gre factors and a high concentration of initiating nucleotide (6). To prove the generality of the branched pathway, I examined the existence of the branched pathway in initiation at the T7A1 promoter. I found that the promoter-arrested pathway exists in initiation at the T7A1 promoter. This finding suggests a generality of the

branched pathway in initiation, which would resolve contradictory observations that have been reported for various promoters.

I next addressed the question whether the branched pathway has physiological significance in *E.coli* cell. The clue is the effect of GreA and GreB on initiation. *E.coli greA* (growth regulator A) gene was first identified as a multi-copy suppressor of a temperature-sensitive mutant of *rpoB* that encode β subunit of RNA polymerase (9), and therefore the product of *greA*, GreA, was speculated to interact with RNA polymerase and to be involved in transcription. In fact, The GreA induces transcript cleavage by elongation-arrested RNA polymerase which retains its transcript with the 3'-terminus deviated from its active site (10). Since the cleavage occurs at active site of the enzyme, this cleavage causes generation of new 3'-terminus at the site, allowing to re-elongation. GreB was isolated as a protein which has activity homologous to GreA. Namely, the GreB induces cleavage and releases longer oligonucleotides up to 9 nucleotides from the 3'-terminus of the transcript while the GreA does up to 2 or 3 nucleotides (11). Since the RNA polymerase alone has a weak activity to cleave the retaining transcript in the absence of nucleoside triphosphate, GreA and GreB are suggested to play their role as a polymerase chaperone and to enhance the intrinsic cleaving activity of the RNA polymerase (12). Based on these observations, the Gre factors are conventionally considered to be elongation factors.

The Gre factors are also known to act on initiation and reduce abortive synthesis accompanied by the transcript cleavage at some artificial promoters such as mutant T7A1 (13), $T5N25_{antiDSR}$ (14) and $\lambda P_R AL$ (6). At the $\lambda P_R AL$ promoter, the Gre factors act on the stage of binary complex and reduce the abortive transcripts by increasing the conversion between moribund and productive subspecies of the binary complex. In the presence of the Gre factors and high concentration of initiation nucleotide, moribund complex is converted into a productive complex before converting into a dead-end complex and therefore most transcription complexes are engaged in productive elongation. These suggest that the Gre factors can regulate transcription level of genes by the branched pathway. If so, disruption of *greA* and *greB* affects transcription level of genes and thus the cell physiology can be disordered. Therefore, I examined the effect of disruption of *greA* and *greB*. I observed growth defect at low temperature or in Mn^{2+}- or Zn^{2+}-containing medium by the disruption. I found that the Gre factors act on initiation and regulate mRNA level of at least 3 genes, *cspA*, *rpsA* and *atp(unc)* gene. At the major promoter of *atp* operon, *atp* promoter, the moribund complex is observed. These findings suggest the universal existence and physiological significance of the branched pathway in *E.coli* cell.

A. Sequential pathway

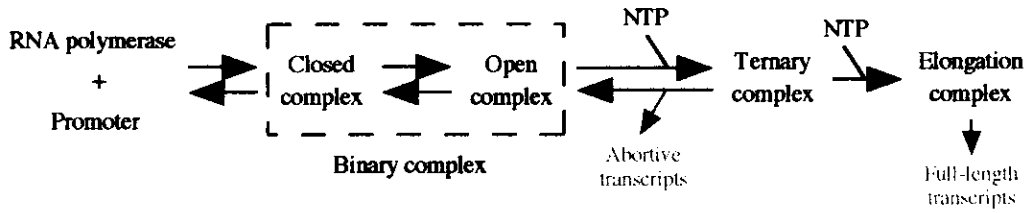

B. Branched pathway

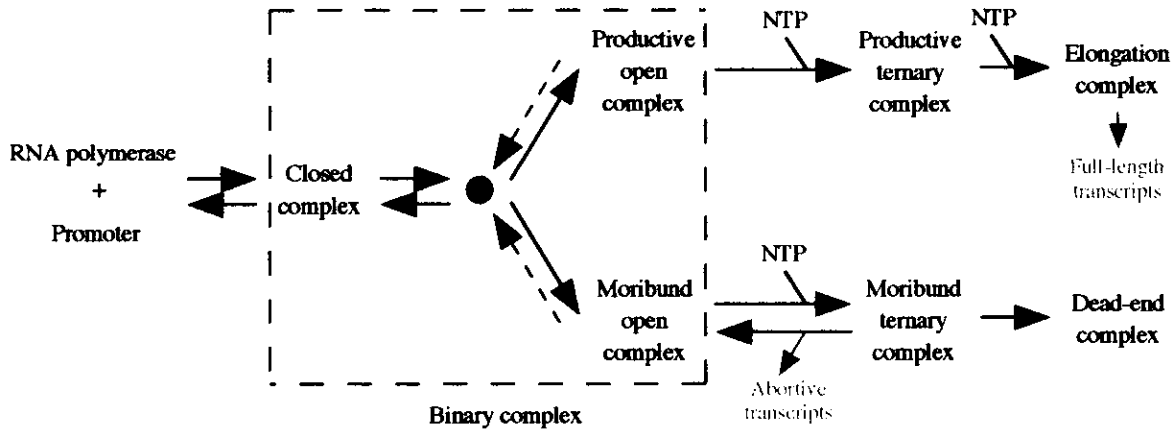

Scheme 1. Two models of the initiation pathway for transcription.
(A) The conventional sequential pathway. (B) The branched pathway that has been applied to the initiation at the λP_RAL promoter. The presence or absence of abortive synthesis in the productive branch has not been determined. The black circle only indicates that a branching point exist on the stage of binary complex. The initiation at λP_RAL with GreA and GreB or at T7A1 promoter in standard salt condition is considered to follow this mechanism with a rapid exchange between binary subcomplexes (the broken arrows). See text for detail.

Results

Moribund complex formation at the T7A1 promoter.

One important line of evidence for the branched pathway at the λP_RAL promoter is the occurrence of persistent abortive synthesis. Since this phenomenon disappears in high salt condition (50 mM Tris-HCl, 10 mM $MgCl_2$, 100 mM KCl, 100 mM NaCl) (3), lower salt conditions may favor formation of the moribund complex. Although little sign of persistent abortive synthesis at the T7A1 promoter has been detected in standard salt condition (50 mM Tris-HCl, 10 mM $MgCl_2$, 100 mM KCl) (3), I decided to test for its occurrence in low salt (20 mM Tris-HCl, 7 mM $MgCl_2$). Transcription from the T7A1 promoter was carried out using a linear 154 bp DNA (Template I in Figure 1A), and produced full-length transcripts (74-mer or longer) together with abortive transcripts (shorter than 12-mer) in the standard salt condition (lane 1 in Figure 1B). Figure 1B also shows that no anomalous reactions take place at low salt (lane 6).

The most sensitive method for detection of persistent abortive synthesis is a pulse-labeling assay (4), in which transcription is started with unlabeled nucleotides and then the labeled initiating nucleotide, [γ-^{32}P]ATP in this case, is added at various time points. In this assay, the amounts of the 5'-end-labeled full-length and abortive transcripts respectively indicate the residual amount of binary complexes that can produce the corresponding transcripts at each time point. Decay of the labeled full-length transcripts in the standard condition was slower than that in the low salt, although the decay of the abortive one is almost the same in the both conditions (Figure 1B). In the sequential pathway, abortive synthesis should precede the full-length synthesis and thus the ratio of abortive to full-length transcripts should not increase in proportion to the reaction time with unlabeled nucleotides. In contrast, this ratio could increase, only when the branched pathway exists and the moribund complex has a longer lifetime than the productive one. The observed ratios for the abortive 4-mer or 10-mer transcripts were plotted in Figure 1C and 1D against the reaction time with unlabeled nucleotides. In the standard salt condition, the ratios slightly increased by maximum 4-fold in 60 sec, whereas they showed marked increases (5-20 fold) in the low salt. These results indicate that persistent abortive synthesis occurs during initiation at the T7A1 promoter by formation of the moribund complex and that deviation from the sequential mechanism is extensive in low salt conditions.

Arrest of RNA polymerase at the T7A1 promoter.

Pulse-labeling provides a catalytic assay, but cannot determine what fraction of binary complex becomes promoter-arrested. This promoter-arrested fraction was therefore measured using an

electrophoretic mobility-shift assay. Promoter-arrested complexes were formed on the 250 bp T7A1 DNA fragment which harbors a *Hae*III site at position +73 (Template II in Figure 1A). To distinguish promoter-arrested from run-off elongation complexes, I removed the unlabeled downstream region carrying any of the latter complexes using *Hae*III digestion. The binary complex was formed in both salt conditions (lanes 4 and 6 in Figure 2A). The observed amount of binary complex formed before nucleotide addition decreased slightly at low salt (Figure 2B, left panel), although DNA-protein complexes in general are stabilized in low salt conditions. On the other hand, the promoter-arrested complex was almost undetectable under standard condition (lane 7 in Figure 2A) but clearly existed in low salt (lane 5), indicating that 2-3% of the binary complex was arrested at the low salt (Figure 2B, right panel). These results suggest that the fraction of RNA polymerase arrested at the T7A1 promoter is small, and that arrest is enhanced at low salt conditions. This result explains why nearly stoichiometric amounts of full-length product are obtained at the T7A1 promoter.

An alternative method to detect the arrested complex is DNA footprinting using exonuclease III (7), which can detect the limits of the region of DNA protected by a bound protein. I thus examined the footprints of RNA polymerase bound to the DNA harboring the T7A1 promoter in both conditions (Figure 3). The DNA was footprinted in the absence of RNA polymerase, or after the formation of binary complex, or after transcription. Heparin was added with the nucleotides to ensure single-round transcription. The footprint on the non-template strand of the naked DNA (lane 2) was the same as that after transcription (lane 4) in the standard condition. This indicates that little RNA polymerase remains at the T7A1 promoter after transcription, in agreement with the results of the mobility-shift assay (Figure 2). In the low salt condition, the footprint of the downstream boundary of the binary complex appears as enhanced bands at positions +9 and +18 to +22 as well as reduced bands at +11 and +13 (lane 7) if compared to naked DNA (lane 6). It should be noted that there is a similar footprint after transcription in the low salt condition, although the bands are relatively faint (lane 8). This indicates that a small fraction of the enzyme is still sitting at the promoter, a conclusion again consistent with that from the mobility-shift assay. These results also suggest that the initiation at the T7A1 promoter is branched and the branch is emphasized in low salt.

There is a difference between the footprints of the binary complexes in the two conditions. In the low salt condition, the downstream edge of the enzyme footprint is at position +22, while it is at +19 in the standard salt condition. (lanes 3 and 7). No difference between the footprints at the upstream boundary was observed between the low and standard conditions (data not shown). The difference at the downstream edge suggests that the RNA polymerase in the binary complex may be more forward-tracked in the low salt condition than in the standard. Alternatively, exonuclease III may push or partially displace RNA polymerase

further upstream in the latter case, so that the observed differences reflect not the true boundaries but rather the elasticity of the downstream edge. Whichever is the case, it is clear that there is a physical difference between downstream boundaries in the two conditions. I will tentatively call the change forward-tracking here. This could result from a structural difference between moribund and productive binary complexes, if the earliest branching point occurs at the stage of binary complex formation, as in the case of the λP_RAL promoter (6).

Detection of binary subspecies by mapping of RNA polymerase catalytic center onto DNA. One of the most important features of the enzyme complex in terms of its enzymatic activity is the location of the catalytic center relative to DNA. Therefore, I examined whether this location shifts in accord with the putative forward-tracking of RNA polymerase which was detected by exonuclease III footprinting. A ferrous ion (Fe^{2+}) is allowed to replace the Mg^{2+} that normally makes a chelate with the catalytic center. The resultant Fe^{2+} chelate generates hydroxyl radicals that cleave DNA template strand nearby, allowing fine mapping of the catalytic center onto the DNA in the two conditions (15). Figure 4 shows the tracings of the autoradiograms obtained by this mapping. The position of the catalytic center of the RNA polymerase-T7A1 promoter complex in the standard condition maps mainly at position –2, with a second lower peak at –1 (the gray line in Figure 4A), while the mapping in the low salt condition indicates significant forward-shifting, such that the two major peaks at –2 and –1 have similar strengths (the black broken line). The direction of the movement detected by the Fe^{2+} cleavage is the same as was suggested by the exonuclease III footprinting. Therefore, the enzyme in binary complex with the T7A1 promoter is very likely to be positioned further forward in the low salt condition. Since lower salt conditions favor formation of the moribund complex, this forward-tracking reflects the formation of a moribund binary complex, supporting the idea that a branching point in the branched pathway exists at the binary stage. The forward-tracking of RNA polymerase at the T7A1 promoter in low salt is in sharp contrast to that at the λP_RAL promoter, where back-tracking of the binary complexes as a response to reduced salt concentration has been observed by the method used here (Figure 4B). These results indicate that the effect of salt concentration on positioning of the binary complex is specific to a promoter.

From these results I concluded that initiation at the T7A1 promoter is branched and thus the branched pathway is more general than the sequential pathway as initiation mechanism. Therefore, I next addressed the question whether the branched pathway has physiological significance in *E.coli*.

Phenotypes of disruptant of *greA* and *greB*.

It is essential to use a genetic tool to know whether the branched pathway of initiation exists in vivo or not. A clue was the finding that GreA and GreB relieve the arrest of RNA polymerase at the λP_RAL promoter, and thus there could be similar action of the Gre factors at authentic promoters of *E.coli*. By this reason, a mutant *E.coli* strain with disrupted *greA* and *greB* genes was constructed by T. Kubori, H. Nagai and N. Shimamoto. To speculate the physiological significance of the branched pathway, I first inspected the phenotypes of the mutant strain. The *greA*$^-$*greB*$^-$ strain grew well on LB-agar plate at 37°C (Figure 5A), however the growth was inhibited at 25°C (Figure 5B). This mutant strain was also sensitive to Mn^{2+} and Zn^{2+} in the LB medium (Figure 5C and 5D). These defects were recovered if the *greA* or *greB*-containing plasmid, pMS002 or pTK003, was introduced into the mutant strain, although the effect of *greB* was weaker than that of *greA*. Since *greA* works as initiation factor rather than elongation factor and *greB* does inverse, this results may indicate that the effect on initiation is major. These imply that transcription regulation by the branched mechanism may have the physiological significance.

Survey of genes regulated by *greA* and *greB*.

To examine whether the Gre factors act as a transcriptional regulator in *E.coli*, we searched the transcription units regulated by the Gre factors by comparing the levels of transcripts between the disruptant and the isogenic wild-type. By using a gene array analysis, Kubori and Shimamoto have identified 206 decreased spots and 67 increased ones upon disruption of both *greA* and *greB* (unpublished result). Since the array analysis was hardly conclusive, I performed Northern analysis of several candidate genes that were selected by the array. The 20 base sequences near the 3'-end of the cistrons were selected as target for the ^{32}P-labeled probes. Among 7 genes examined, *atpC*, *cspA* and *rpsA*, clearly showed the expected decrease in the amount of mRNA (Figure 6). The observed levels of the decrease by the disruption were 60-80%, indicating that transcription of these genes is indeed regulated by the Gre factors in *E.coli*.

Effect of GreA and GreB on transcription initiation at the *E.coli* authentic promoters.

To examine whether the Gre factor-mediated transcription regulation is carried out by the branched pathway, I investigated the effect of the Gre factors on initiation by using in vitro transcription assay. DNA templates used in this experiment were prepared by PCR using DNA fragments from Kohara's library (16) (Figure 7A). Each template contains an authentic *E.coli* promoter reported previously (17, 18, 19, 20). If two or more promoters exist, the major promoter(s) were selected. Transcripts were internally labeled with [α-^{32}P]UTP because of amplification of signals from transcripts. Transcription from the selected promoters produced a few amounts of full-length transcripts in the absence of GreA and GreB (Figure 7B). However,

the amounts increased to 2-6 fold in the presence of GreA and/or GreB. The observed increase of the full-length transcripts is consistent to the result obtained for the λP_RAL transcription unit that gave 3-4 fold increase of full-length transcripts (6). Although abortive transcripts seemed to be increased by addition of GreA or GreB, the apparent increases were thought to be due to accumulation of cleaved transcripts generated by the cleavage of long transcripts at 3'-position. In fact, abortive transcripts whose positions do not overlap with the cleaved one were decreased by the addition of Gre factors. The increase of the full-length transcripts accompanied by the decrease of the abortive one was confirmed by another in vitro transcription assay where transcripts were 5'-end-labeled with [γ-^{32}P]ATP or [γ-^{32}P]GTP and thus no cleaved transcript was observed (Figure 7C). The Gre factors can work as elongation factors relieving transcriptional pause (10, 11). However, no significant decrease of the pause was observed. These indicate that the Gre factors act on transcription initiation at these transcription units rather than elongation and increase the amount of full-length transcripts. Among the promoters tested, *atp* promoter was examined most detail.

Effect of disruption of *greA* and *greB* on transcription from the *atp* promoter.

Because several minor promoters exist near the *atp* promoter (17, 18), the results of the Northern analysis of *atpC* gene does not necessarily indicate the existence of its activation at the promoter by the Gre factors. To examine whether the *atp* promoter is responsible for the activation by the Gre factors in vivo, I carried out a primer extension analysis. The primer for this assay, atpIp-ds primer, has a sequence complementary from +40 to +59. For an internal control of the primer extension assay, another primer, metY-R1 primer, was designed to hybridize to 5'-UTR of *metY* mRNA (from +28 to +47 position). Northern and primer extension analyses using this promoter showed that the disruption of *greA* and *greB* did not affect the amounts of *metY* transcript (data not shown). The result of the primer extension assay (Figure 8A) showed a single start site for the *atp* mRNA, although the position is one base upstream from that reported previously (21), which could be interpreted as an extra-elongation artifact of the reverse transcriptase. This transcript decreased to 60% by disruption of *greA* and *greB* (Figure 8B). This decrease was almost recovered by the presence of an expression plasmid expressing *greA* or *greB*, while introduction of pBR322 affected only slightly (Figure 8B). These results confirm that the *atp* promoter is indeed a target for the GreA and GreB action in vivo.

Moribund complex formation at the *atp* promoter/

The Gre factors are known to relieve promoter-arrest at the λP_RAL promoter by introducing the rapid exchange between the moribund and productive species (6). Since the Gre factors give

the same gross effect on the *atp* promoter as the λP_RAL promoter, moribund complex is expected to be formed at the promoter. To examine this possibility, I performed pulse-labeling assay, the procedure of which is described above. Ratio of abortive (5-mer and 7-mer) to full-length transcripts increased to 2-3 fold in 60 min after the addition of unlabeled nucleotides (Figure 9), indicating that persistent abortive synthesis occurs at the promoter. This result indicates that the moribund complex is generated at the *atp* promoter, an authentic promoter of *E. coli*.

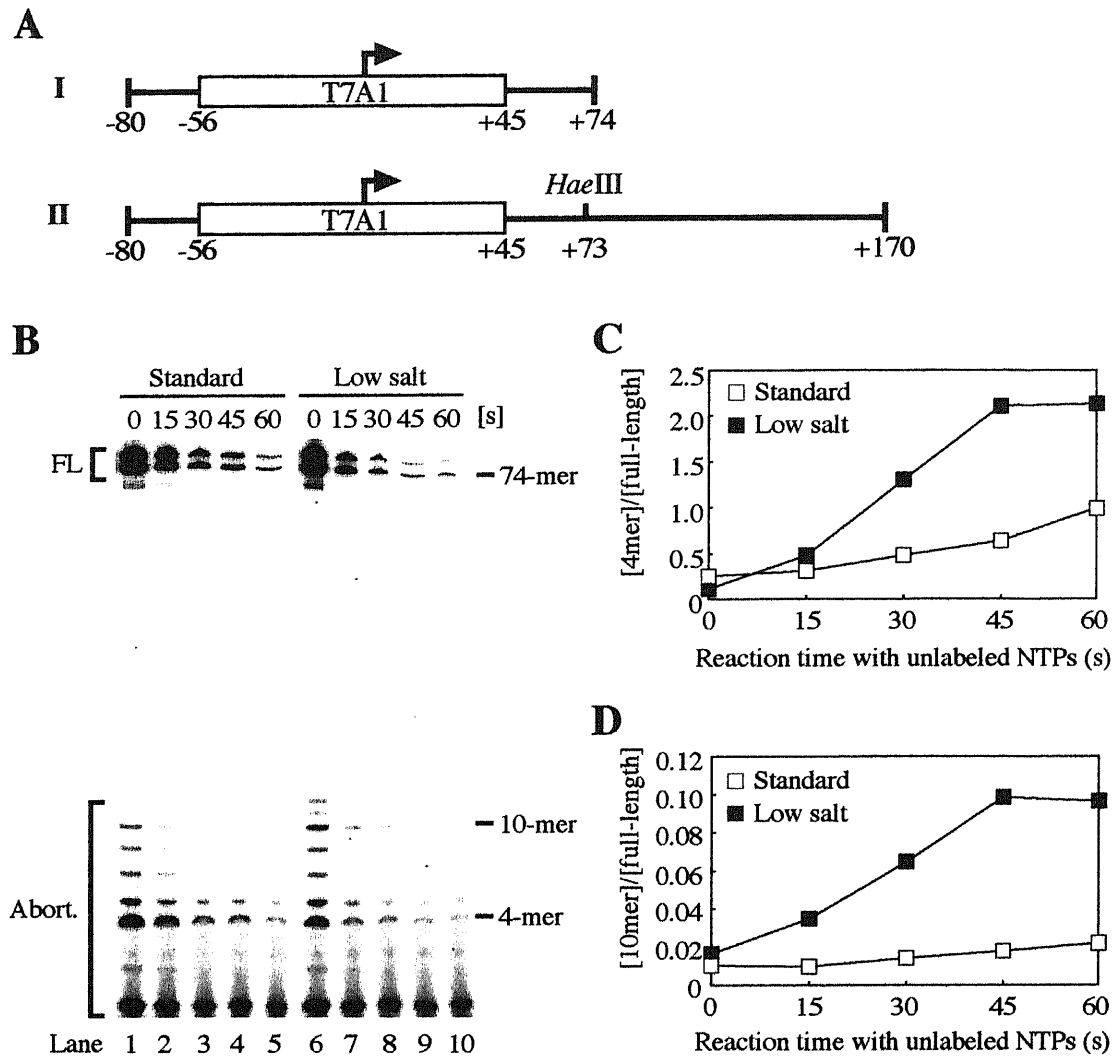

Figure 1. Pulse-labeling experiments in standard and low salt conditions.
(A) The template DNAs used in the T7A1 study. The arrows indicate transcription start sites. The boxes indicate the region derived from T7 DNA containing the A1 promoter and the transcription start site. Template I was used in the kinetic and footprinting assays and template II was in the mobility shift assay. (B) Pulse-labeling assay. ^{32}P-labeled transcripts were synthesized in the standard or low salt condition and separated in a 20% sequencing gel. The numbers above the autoradiogram indicate the reaction time with unlabeled NTPs. (C, D) The ratios of the amounts of 4-mer (C) and 10-mer (D) to that of full-length product plotted against the reaction time with unlabeled NTPs. The filled and open squares represent data in the low and the standard salt conditions, respectively.

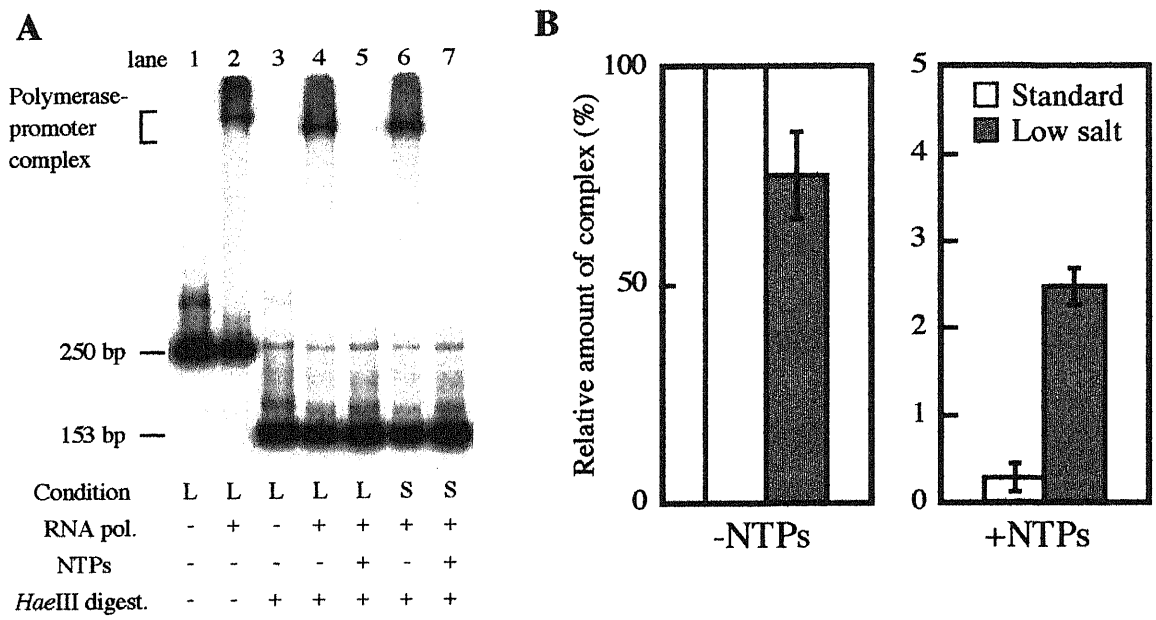

Figure 2. Detection of promoter-arrested complexes by Gel shift assay.
(A) Autoradiogram of the gel. The 250 bp fragment with ^{32}P-labeled non-template strand was incubated with RNA polymerase and the indicated reactions were carried out. L and S indicate that these assays were carried out in the low and standard salt conditions, respectively. The products were electrophoresed in 5% polyacrylamode gel. (B) The amounts of RNA polymerase-promoter complexes observed as shifted-band (153 bp + RNA polymerase) were quantified. Relative amounts of the complexes in the standard (white bars) and low (gray bars) salt conditions are indicated. The amount of the RNA polymerase-promoter complex formed before NTP addition (binary complex) under standard condition was set to 100%.

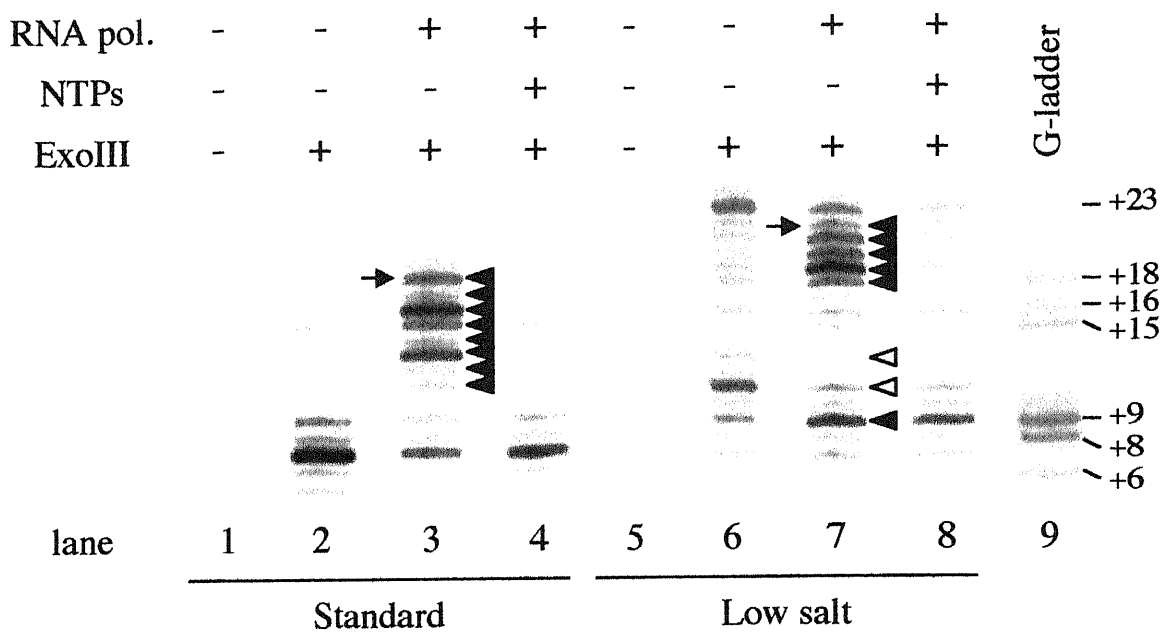

Figure 3. Detection of promoter-arrested complexes by Exonuclease III-mediated DNA footprinting.

The 5'-end of the non-template strand of the DNA harboring the T7A1 promoter was labeled with ^{32}P and footprinted after the reactions indicated. Positions on DNA are indicated relative to the transcription start as +1. Digestion of the DNA was carried out in the absence (lanes 2 and 6) or presence (lane 3 and 7) of RNA polymerase, or after completion of transcription by addition of nucleotides and incubation for 20 min (lanes 4 and 8). The reactions were performed in standard (lanes 1-4) and low (lanes 5-8) salt conditions. Open and filled triangles respectively indicate the bands with decreased or increased intensities upon formation of binary complex. Arrows indicate the downstream edge of the footprint of binary complex.

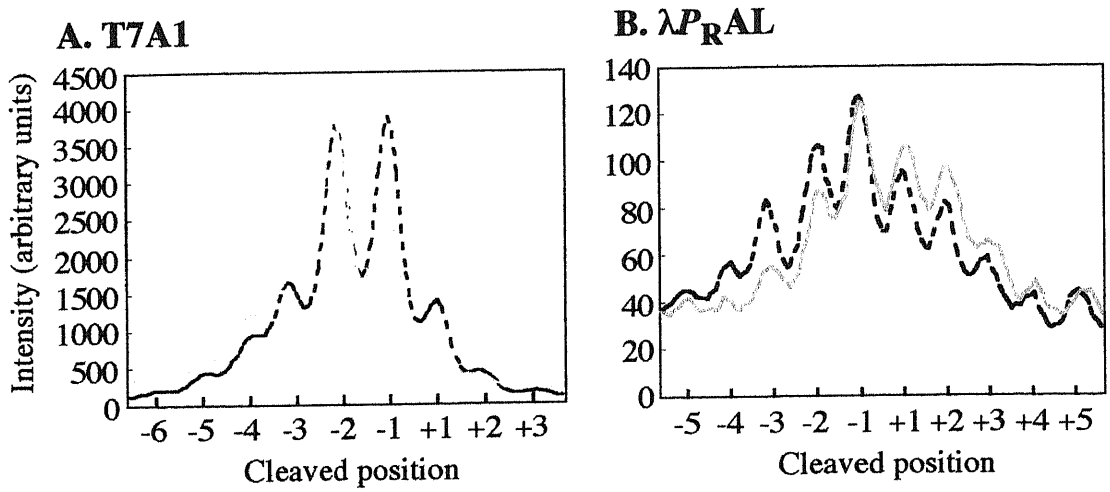

Figure 4. Intensity profiles of DNA footprints produced by Fe^{2+}-induced radical cleavage at catalytic center of RNA polymerase.

The profiles of band intensities of the template strand are shown for the T7A1 promoter (A) and the λP_RAL promoter (B). The broken and gray lines respectively indicate the cleavage in lower and higher salt conditions. Cleaved positions are indicated relative to the transcription start site as +1.

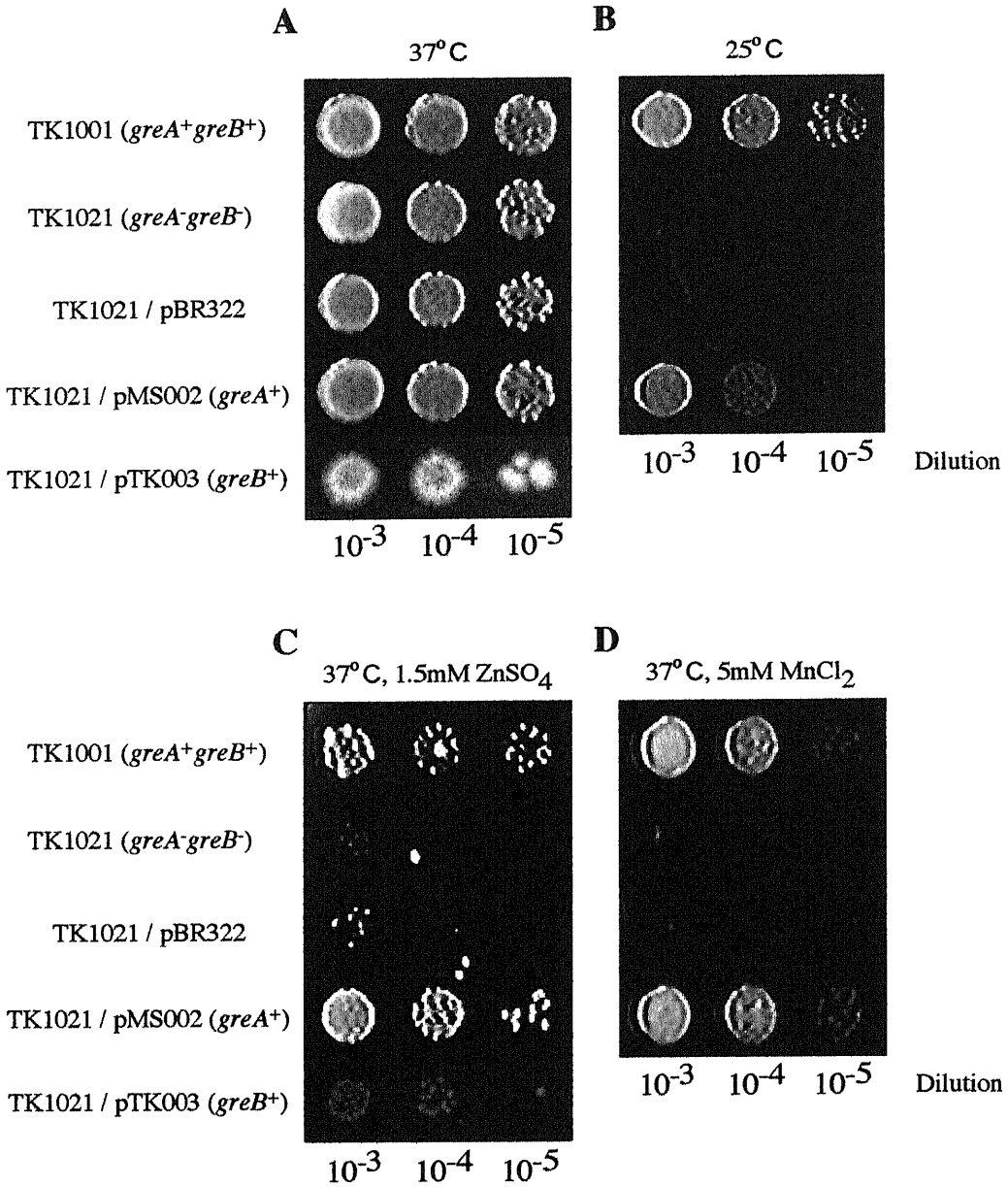

Figure 5. Growth defect of *E.coli greA-greB-* strain.
Overnight culture of each strains was diluted and spotted onto the LB (A, B), LB+1.5 mM $ZnSO_4$ (C) and LB+5 mM $MnCl_2$ (D) plates. These plates were incubated at 37°C (A, C, D) and 25°C (B) for 24 hours. Line 1, *E.coli* TK1001 strain (*greA+greB+*); line 2, *E.coli* TK1021 strain (*greA-greB-*); line 3, TK1021 harboring pBR322 which contains no *gre* gene; line 4, TK1021 harboring the *greA*-containing pBR322 derivative (pMS002); line 5, TK1021 harboring the *greB*-containing pBR322 derivative (pTK003). The TK1021 harboring pTK003 was also viable on LB plate at 25 °C and on LB+5 mM $MnCl_2$ plate at 37 °C, but the growth was slightly inhibited if compared to the TK1001 (T. Kubori and N. Shimamoto, unpublished result).

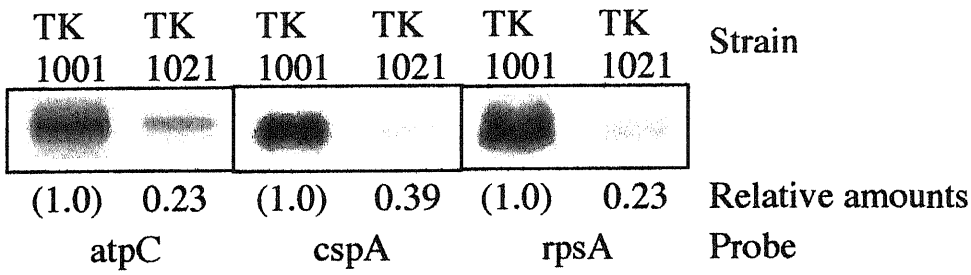

Figure 6. Effect of *greA* and *greB* on transcription of *atpC*, *cspA* and *rpsA* genes, revealed by Northern blot analysis.

The amounts of transcript from *E.coli* TK1021 strain ($greA^{-}greB^{-}$) are indicated as ratios to the amounts from *E.coli* TK1001 ($greA^{+}greB^{+}$).

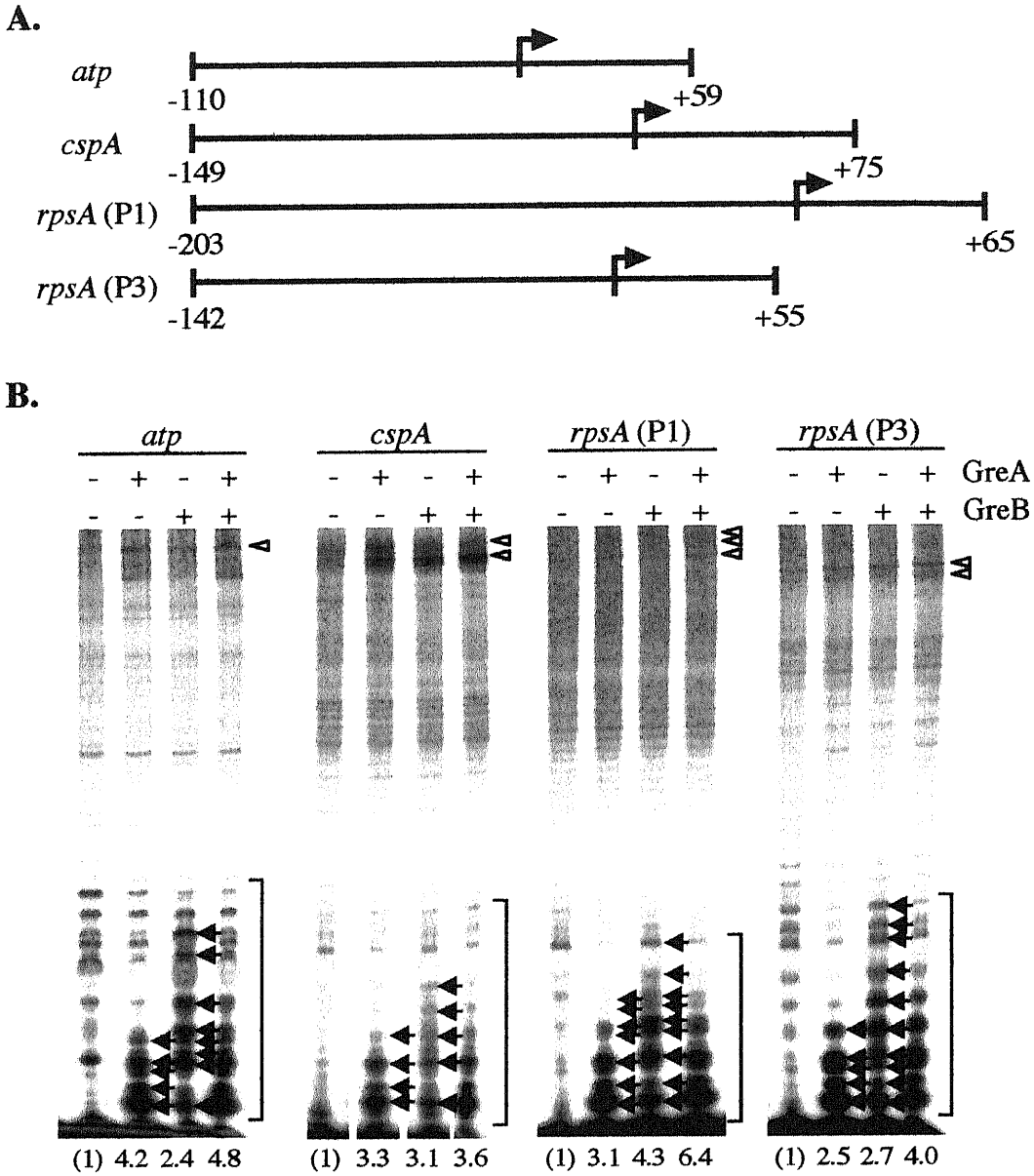

Figure 7. Effect of GreA and GreB on in vitro transcription from the promoters. (A) The template DNAs used in this experiment. The arrows indicate transcription start sites (+1). Two templates were prepared for examination of *rpsA* because there are two major promoters, P1 and P3, in front of the gene. (B,C) Transcripts synthesized on the DNA templates in the absence or presence of the GreA and GreB. The transcripts are internally labeled with [α-^{32}P]UTP (B) or 5'-end-labeled with [γ-^{32}P]GTP or ATP (C). Open triangles indicate positions of full-length transcripts. Brackets and arrows indicate putative abortive transcripts and cleaved RNAs, respectively. The amounts of full-length transcripts are indicated below the autoradiograms as ratios to the amounts observed in the absence of GreA and GreB.

C.

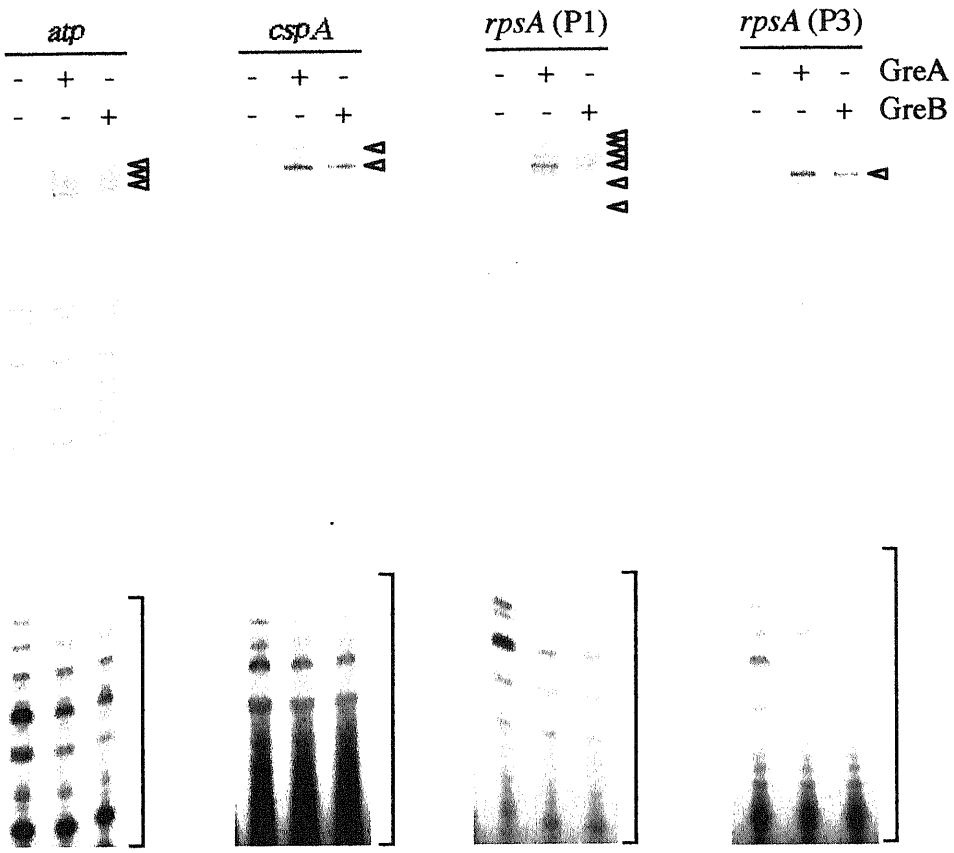

Figure 7. (Continued)

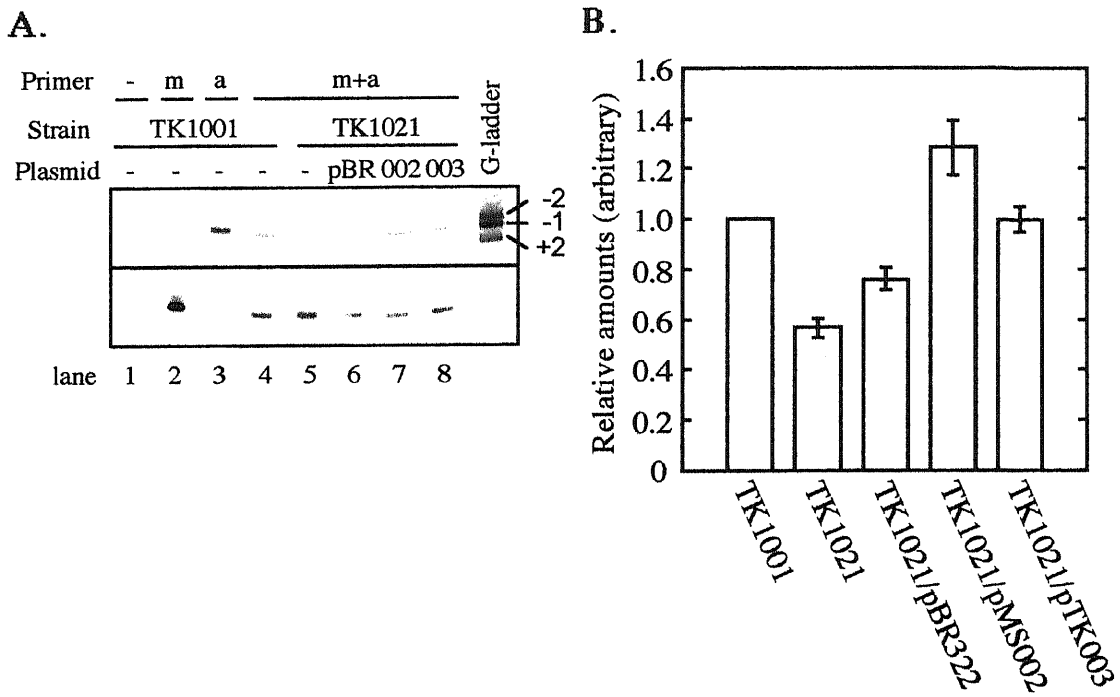

Figure 8. Quantitation of transcripts from *atp* promoter by primer extension. (A) Autoradiogram of the gel. Total RNAs were extracted from *E.coli* TK1001 (*greA*$^+$*greB*$^+$) and TK1021 (*greA*$^-$*greB*$^-$) strains. "a" and "m" on top of the gel respectively indicates atpIp-ds and metY-R1 primers used in this experiment. Positions are indicated relative to the transcription start site taken as +1. The *greA*- and *greB*-containing plasmids, pMS002 and pTK003, are indicated as 002 and 003, respectively. (B) Amounts of transcripts from *atp* promoter. The amounts of *atp* transcript are normalized by that of *metY* transcript. Then the relative amounts of the normalized transcript are calculated as ratios to the amounts observed in the case of TK1001.

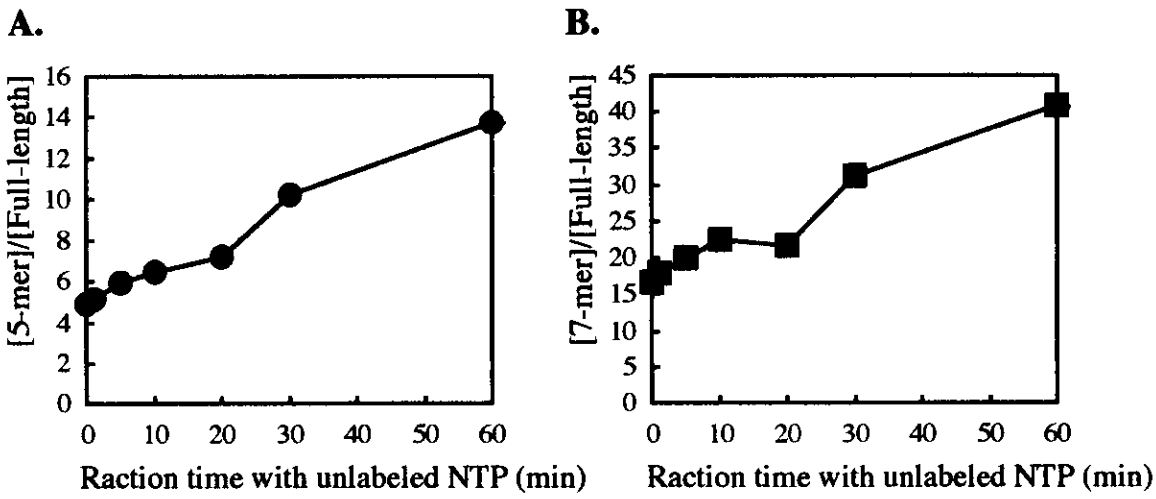

Figure 9. Pulse-labeling experiment in initiation at *atp* promoter.
The ratios of the amounts of 5-mer (A) and 7-mer (B) to that of full-length product plotted against the reaction time with unlabeled NTP.

Discussion

Generality of branched pathway mechanism.

Among many promoters for *E. coli* RNA polymerase, the A1 promoter of bacteriophage T7 (22) has been one of the best studied in vitro, because it has a high affinity for the enzyme (2, 23) and is among the strongest (24). Using this promoter, the order of binding of substrates (2) and the rate of incorporation of single nucleotide were determined (2, 23), as well as the characteristics of abortive synthesis (25, 26). The concepts of promoter clearance (24) and of initial transcribing complex/initial elongating complex (27) were established by experiments on promoters including T7A1, and the translocational movement of RNA polymerase away from this promoter was systematically studied (28, 29). In addition to these normal features of transcription, elongation-arrest was first discovered in the T7A1 transcription unit (30), and hydrolysis of transcripts was also revealed (31, 32). Therefore, the T7A1 promoter is the most representative promoter used in kinetic studies of transcription by *E. coli* RNA polymerase. All the kinetic results obtained have been interpreted based on the assumption that the mechanism of initiation at this promoter is sequential.

However, I have presented two lines of evidence that initiation at the T7A1 promoter follows the branched pathway, which has recently been established for other promoters such as λP_RAL, *lac*UV5 (4), and the *malT* promoter (8). The kinetic evidence is the existence of persistent abortive synthesis shown by a highly sensitive assay, pulse-labeling assay, and the biochemical evidence, the existence of arrested complexes detected by mobility-shift and exonuclease III footprinting assays. By using the pulse-labeling assay, I was able to detect persistent synthesis of normal abortive transcripts in the standard buffer containing 100 mM KCl, although a conventional kinetic assay detected persistent synthesis only for a misincorporation product (with A instead of G at the fourth position) at 50mM NaCl (31). Because persistent abortive synthesis has also been observed at the λP_RAL and *lac*UV5 promoters (4), I conclude that there is no qualitative difference between initiation at the T7A1 promoter and the others. The difference is only quantitative. The observed common features suggest that the branched pathway is general among the promoters for σ^{70}-holoenzyme of *E.coli* RNA polymerase.

In view of the common features, I am inclined to hypothesize that the earliest branching point of the reaction pathways exists at the stage of binary complex for the T7A1 promoter, as already established for the λP_RAL promoter. This hypothesis is substantiated by the results of DNA footprinting with Exonuclease III and for Fe^{2+}-induced cleavage at the catalytic center. In the low salt condition, a significant fraction of binary complex is forward-tracked at the T7A1 promoter and the footprint of the binary complex agrees with that of the promoter-arrested

complex obtained after RNA synthesis. This agreement suggests that the forward tracking of the footprint is due to the formation of a significant amount of moribund binary complex. Since the fraction of complex arrested after transcription is only 2-3%, the major fraction of binary complex formed at an early stage is likely to be converted into productive complex during RNA synthesis.

At the T7A1 promoter, almost no dead-end complex is formed in the standard salt condition. This result means that the precursor of the dead-end complex, moribund complex, is converted into a productive complex more rapidly than it is inactivated as the dead-end one. Therefore, in the standard salt condition, the productive and moribund subspecies formed at the T7A1 promoter are expected to be rapidly exchanging, while those at the λP_RAL promoter are formed essentially without the exchange (7). While it is difficult to directly measure the conversion rates, we can observe the total dissociation process that is composed of the exchange reaction and the breakdown of binary complex. In the standard salt condition, the total dissociation process at the T7A1 promoter is expected to be more rapid than that at the λP_RAL promoter. In fact, the reduction of the arrest at the λP_RAL promoter accompanies acceleration of the total dissociation process in both cases of the mutation in σ factor (3) and the presence of the Gre factors (6). In the former case, a biphasic dissociation kinetics was actually observed, indicating that one of the phase is the interconversion and the other is the breakdown. In the latter, however, the dissociation kinetics is almost monophasic, indicating that one of the steps is too rapid to be measured. We observed that in the case of the T7A1 promoter the dissociation kinetics are monophasic for full-length and 6-mer species and the rate constants are the same, 0.2 min^{-1}. (33). These are much larger than that for initiation at the λP_RAL promoter, 0.03 min^{-1} for full-length and 9-mer species (3). This rapid and monophasic decay at the T7A1 promoter is consistent with the expected rapid interconversion of the subspecies of binary complex.

Structural aspects of the moribund complex.

Mutations in region 3 of σ^{70}, which is major σ factor and is required for recognition of a class of promoters, are known to alter the level of abortive transcription (34). The alteration is due to an increase of reversibility between the binary complexes (3). According to protein footprinting of σ^{70}, this region is protected in free enzyme as well as binary complex but exposed in the promoter-arrested complex at the λP_RAL promoter (35), indicating that the structure of this region changes upon the formation of moribund complex. The region binds to core enzyme (35, 36) and lies in close proximity to the site between –10 and –35 box and at the transcription start site (+1) (37). In fact, these features have been confirmed to exist in the crystal structure of the complex of *T. aquaticus* RNA polymerase with a promoter DNA complex, where the region 3 binds to the putative exit channel for RNA (K. Murakami and S.A. Darst. unpublished result).

All these results suggest that structural changes in this part of the binary complex alter interaction between DNA and RNA polymerase, and determine the fates of the binary complex.

I consistently observed that location of catalytic center in binary complex shifts according to change of salt concentration which attributes to stability of the moribund complex, although the shift has opposite direction for T7A1 and λP_RAL promoters. Although the different direction is hardly explained from simple comparison of DNA sequences of the promoters, speculations are possible. In one model, moribund subspecies does not escape from a promoter, because it binds more stably than productive one. If the active site of the most stable binary subspecies locates between the position near –1, the position of the binary species at the T7A1 moves forward according to the increase of moribund subspecies at low salt, because the less stable productive subspecies has the position mainly at –2, as shown in the standard condition. At the λP_RAL promoter, however, the position in the productive species is +1 or more, and thus the average position goes backward at low salt. Other models are equally possible. Irrespective of the models for moribund complex, the tracking should not be understood as a whole movement of RNA polymerase molecule but rather be accepted as distortion of the complex, because the upstream boundary is not moving.

Explanation of atypical features of the T7A1 promoter.

In spite of its widespread use in kinetic studies, the T7A1 promoter is not necessarily a typical one functionally. The T7A1 promoter directs the synthesis of full-length products much more efficiently than other promoters. It has been suggested that full-length transcript formation is stoichiometric with the amount of preformed binary complexes at the T7A1 promoter, but not at other promoter (5). In other words, the high efficiency is due to conversion of almost all binary complexes, whereas at other promoters only a fraction of complexes achieve elongation the rest being excluded. Indeed the nearly full conversion to elongation complexes was confirmed for the T7A1 promoter by the results of DNA footprinting and mobility shift assays in this study. In contrast, only a quarter to half of all binary complexes clears the λP_RAL promoter (5, 6).

Action of GreA and GreB in initiation at authentic promoters of *E.coli*.

It is previously reported that the Gre factors reduce abortive synthesis and enhance full-length synthesis at some artificial promoters such as mutant T7A1 (13), T5N25$_{antiDSR}$ (14) and λP_RAL (6). The action of the Gre factors at the λP_RAL promoter is explained by the branched pathway, because they mitigate the promoter arrest and increase full-length transcripts in the presence of high concentration of initiation nucleotide. In the T5N25$_{antiDSR}$ study, Hsu and coworkers demonstrated that GreA and GreB increase the amount of full-length transcript from this promoter accompanied by cleavage of anomalous abortive transcripts of 13 to 16-mer (14).

Chan and Gross suggest, according to the sequential pathway, that the activation at this promoter by Gre factors is due to avoiding the kinetic trap of synthesizing the anomalous transcripts, which is thought to be generated by inappropriate interaction between the transcript and the RNA polymerase (38). However, it can also be explained that the complex with the anomalous transcripts is a moribund complex and the reaction pathway is branched similarly to the one at the λP_RAL promoter. If the presumed moribund complex slowly converts into productive complex rather than being inactivated to produce the dead-end complex, the slow conversion constitutes a kinetic trap, the escape from which is accelerated by the Gre factors.

I here report that the Gre factors activate the initiation at the *atp*, *cspA* and *rpsA* promoters and that transcripts of these genes are decreased by *greA* and *greB* disruption. These indicate that the Gre factors actually work in initiation not only at the artificial promoters but also at the authentic promoters of *E.coli*. A pulse-labeling experiment revealed the formation of moribund complex at the *atp* promoter, suggesting that the action of the Gre factors at this authentic promoter is also explained by the branched pathway. These findings also claim that the Gre factors are bonafide initiation factors, although they were discovered as elongation factors that mitigate elongation arrest in vitro.

A putative role of GreA and GreB in transcriptional regulation of *atp* operon.

The *atp(unc)* operon is composed of nine genes. The first of these, *atpI*, encodes a protein of unknown function and the remaining eight genes, *atpBEFHAGDC*, encode subunits of the membrane-associated proton-translocating ATP synthase (H^+-ATPase). The *atpBEF* and the *atpHAGDC* genes encode respectively abc subunits (comprising membrane-integrated F_o sector) and $\delta\alpha\gamma\beta\varepsilon$ subunits (comprising F_1-ATPase sector). Relative expression level of these genes should be regulated by RNA processing followed by RNA degradation and by translational efficiency of each gene, because the newly synthesized subunits have to be assembled into a complex with the stoichiometry $\alpha_3\beta_3\gamma_1\delta_1\varepsilon_1 a_1 b_2 c_{12}$. Thus, these post-transcriptional events have been well investigated (reviewed in ref. 39).

On the other hands, transcriptional regulation of the operon, which is considered as regulation of total amount of the complex, is less investigated. There are one major promoter (the *atp* promoter) upstream of the *atpI* gene and two minor promoters in the *atpI* gene (17, 18). Kasimoglu and coworkers reported that level of the transcript from the major promoter in vivo varies less than threefold in various growth media with different availabilities of electron acceptors, carbon compounds, or the pH of the culture medium (40). Furthermore, In *E.coli* there is no factor known so far regulating transcription from the *atp* promoter in response to environmental conditions. These suggest that the expression level of the ATPase complex is maintained constitutively. Therefore, the fact that GreA and GreB activate transcription from

the promoter suggests that these factors guarantee constitutive transcription of the operon by preventing inactivation of the RNA polymerase at the promoter, rather than activate the transcription in response to the environmental conditions.

Universal existence of the branched pathway in *E.coli* cell.

The first implication of the existence of the branched pathway in vivo was found in the study of stringent control of transcription, the response to the starvation of amino acids. The critical factors for this control are guanosine tetraphosphate, ppGpp, and pentaphosphate, pppGpp, which are synthesized by the products of *relA* and *spoT*. The mutant strain of these genes cannot grow on an agar plate containing minimal medium, unless it gains an oxotrophic mutation. Two of such mutations are mapped in the *rpoD* gene encoding σ^{70} (41). Since they are mutations in σ^{70}, they alter the nature of transcription complex in initiation. Since one of the speculated mechanism for the ppGpp and pppGpp action is dissociation of RNA polymerase from a stringent promoter, the enzyme with the mutant σ^{70} would dissociate from a promoter more rapidly than the wild-type enzyme. This was actually proved in vitro by using the mutant σ^{70}-RNA polymerase and the λP_RAL promoter (3). Since this rapid dissociation cancels accumulation of the moribund species of binary complex (3), the nature of the *rpoD* mutants suggests the existence of the branched pathway in initiation at a promoter.

The second implication was the action of CRP on the *malT* promoter. It has been reported that expression of *malT* is controlled by *crp* in vivo (42). Initiation at its promoter had been known to be activated by the product of *crp*, CRP. Addition of CRP-cAMP to the purified reconstituted transcription system showed an enhancement of full-length transcript (8). Furthermore, when CRP is removed from pre-formed CRP-RNA polymerase-promoter complex, the residual polymerase-promoter complex is still productive (8). These indicate an action mechanism of the CRP that this does not control a rate-limiting step in the initiation pathway but determines fate of the RNA polymerase-*malT* promoter complex, productive or non-productive, probably by changing its conformation. This mechanism seems to fit to a branched pathway model, that is, non-productive branch exists in initiation at the *malT* promoter and the CRP mitigates the formation of non-productive species.

From the in vitro and in vivo studies of the Gre factors, I here present the third implication of the existence of the branched pathway in *E. coli*. Northern blotting and primer extension assay consistently indicated that the transcript of *atp* operon decreased in the cells with disruption of *greA* and *greB*. In vitro reconstituted system composed of purified components showed that this decrease was reproduced and that the change is in the initiation at the *atp* promoter but not the other steps of elongation. These suggest that the Gre factors activate transcription by mitigating promoter arrest of RNA polymerase at the *atp* promoter. The Gre

factors also increase transcripts of *cspA* and *rpsA* in vivo and reduce the abortive transcripts at their promoter in vitro, suggesting that the action of the Gre factors at these promoter is similar to that at the *atp* promoter. These observations support the universal existence of the branched pathway in *E.coli* cell.

A possible role of the branched pathway in *E.coli*.

Disruption of *greA* and *greB* of *E.coli* causes growth deficiency at 25 °C, or in Mn^{2+} or Zn^{2+}-containing LB medium, implying that transcriptional regulation by the Gre factors is responsible for adaptation to the various environmental conditions. In fact, the disruption reduces mRNA level of genes coding a cold shock protein, CspA (Figure 6). Northern analysis of genes which contribute to Zn^{2+} tolerance revealed that transcription of *zraP*, which encodes a Zn^{2+}-binding protein and required for Zn^{2+} tolerance, is decreased by the disruption (M. Susa and N. Shimamoto, unpublished result). Therefore, the branched mechanism may be needed for the adaptation.

Physiological significance of the branched pathway.

Both the branched and sequential pathways could control the level of transcription in the multiple-round transcription that occurs in vivo. However, there are two distinct characteristics that are specific to the branched pathway. The formation of dead-end complex attenuates the level of transcription irrespective of the location of the rate-limiting step in transcription initiation, whereas in the sequential pathway, kinetic control is effective only at the rate-limiting step (Figure 10A). Therefore, initiation could be regulated by the branched pathway even if the rate-limiting step changes according to the physiological environment. The second special characteristic of the branched pathway is persistent repression (Figure 10B). If a repressor inactivates RNA polymerase-promoter complex by the branched pathway, the inactivation could be maintained long after dissociation of the repressor, and the promoter could remain blocked until the arrest was relieved. Such persistent repression causes saving of copy number of the RNA polymerase, because the initiation arrest would not generate a queue of RNA polymerases in the transcription unit, which would be expected if regulation were due to an arrest in elongation (Figure 10C). It is speculated that the branched pathway is used for transcription regulation in the *E.coli* cell because of these characteristics.

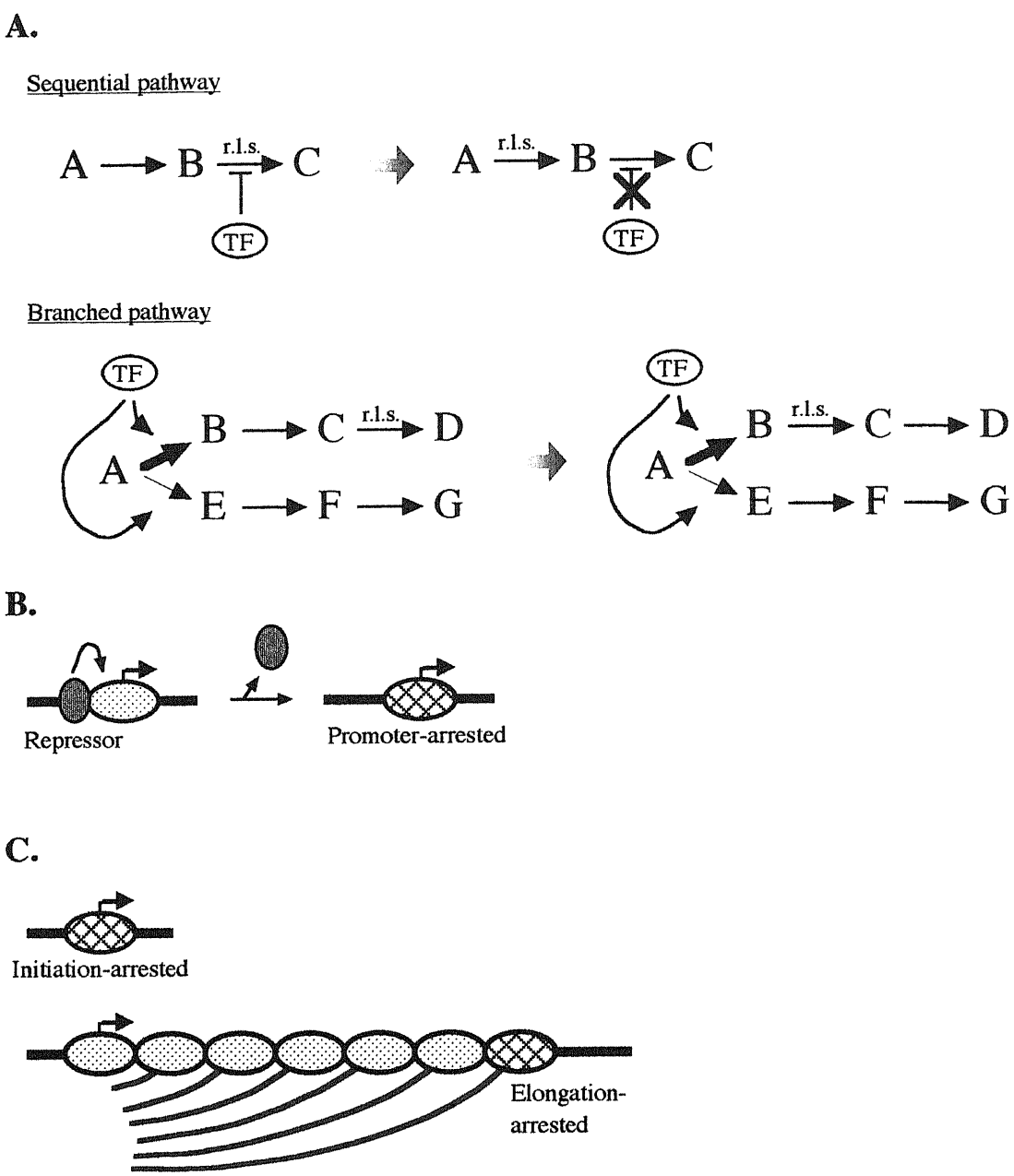

Figure 10. Physiological significance of the branched pathway.
(A) In the sequential pathway, a kinetic control by a transcription factor (TF) is effective only at the rate-limiting step (r.l.s.), and the factor no longer control if rate-limiting step changes according to the physiological environment. On the other hand, in the branched pathway a transcription factor which determines the ratio of amount of "B" to "E" can work irrespective of the position of the rate-limiting step. (B) Persistent repression. If a repressor inactivates RNA polymerase-promoter complex by arresting it at a promoter, the inactivation could be maintained after the repressor dissociates from the operator, and the promoter would remain blocked unless the arrest was relieved by an activator. (C) The arrest during elongation generates a queue of RNA polymerases in the transcription unit, while the arrest at a promoter does not, saving the copy number of RNA polymerase.

Materials and Methods

Materials

Oligo DNAs were purchased from Amersham Pharmacia Biotech K.K. or Genset K.K. Their sequences are shown in Table 1. Nucleotide triphosphates were purchased from Yamasa. [γ-^{32}P]ATP, [γ-^{32}P]GTP and [α-^{32}P]UTP were purchased from New England Nuclear. Restriction enzymes were purchased from Takara Shuzo Co., Ltd. or New England Biolabs Inc. Other chemicals were purchased from Wako pure chemical industries Inc., Nacalai Tesque Inc. and Kanto kagaku Co., Ltd.

Strains and Plasmids

E.coli strains and plasmids are listed in Table 2. These, except pMS001 and pMS002, were gifted from Dr. T. Kubori. For construction of *greA*- and *greB*-containing plasmid, pMS001, *greA*-containing 1.9 kbp *Msc*I-*sal*I fragment from Kohara's clone (16) was cloned into the corresponding sites of pTK003. A *greA*-containing plasmid, pMS002, was prepared as follows. The pMS001 was digested with *Eco*RI and *Bam*HI to remove *greB*-containing 3.2 kbp fragment and then the remaining 5.1 kbp fragment was circularized by using blunting and ligation kit (Blunting high, Toyobo).

Labeling of oligo DNA

0.12 nmol of oligo DNA was incubated at 37 °C for 30 min in 30 μl solution containing 1x reaction buffer (50 mM Tris-HCl (pH7.5), 10 mM $MgCl_2$, 5 mM DTT), 720 μCi [γ-^{32}P]ATP and 20 units of T4 polynucleotide kinase (Takara). The labeled DNA was purified by passing it through a Sephadex G-25 spin column (Amersham Pharmacia Biotech K.K).

Preparation of DNA templates

DNA templates were amplified by polymerase chain reaction (PCR) as follows: 100 μL of Reaction mixture containing 1.6 ng of template DNA, 0.2 μM primers, 0.2 mM dNTP mixture, 1x Z-Taq buffer and 2.5 units of Z-Taq DNA polymerase (Takara) was prepared. Combinations of the template and primers are listed in Table 3. The mixture was incubated at 98 °C for 2 min, and then 30 cycles of thermal change (98 °C for 5 sec then 68 °C for 20 sec) were performed by thermal cycler (Perkin Elmer). After post-incubation at 68 °C for 2 min, the mixture was placed at 4 °C. If the PCR product is heterogeneous, the mixture was subjected to electrophoresis in a 5% polyacrylamide gel in 1x TBE. The gel was stained by Ethidium bromide and a gel fragment containing objective DNA was picked up. This gel fragment was crushed and

incubated with TE buffer containing 1 M NaCl to extract the DNA from the gel into the buffer. After removal of the crushed gel by filtration, the solution was concentrated by Centriprep 10 (Amicon). If the PCR product is homogeneous, the product is purified by using PCR rapid purification system (GibcoBRL). Concentration of the final solution was measured by UV spectrometer (JASCO) as OD_{260}. For preparation of end-labeled DNA, the primer was radio-labeled prior to PCR reaction. Immobilized templates were prepared as follows. Biotinated DNA was mixed with Avidin-coated resin (47) in a buffer containing 10 mM Tris-HCl (pH7.9), 1 mM EDTA and 0.5 M NaCl. The mixture was incubated at 4 °C for more than 12 hours and then the resin was washed with the same buffer for more than 3 times. Bound DNA was estimated by subtracting the input from the unbound DNA.

Pulse-labeling experiment

In Figure 1, at standard salt condition, RNA polymerase and DNA harboring a promoter (final 30 nM each) were pre-incubated for 10 min at 37 °C in reaction mixture containing 50 mM Tris-HCl (pH 7.9), 10 mM $MgCl_2$, 100 mM KCl, 0.15 mg/ml partially hydrolyzed casein and 1 mM DTT. At low salt condition, KCl was omitted and concentrations of the Tris-HCl and $MgCl_2$ were decreased to 20 mM and 7 mM, respectively. Substrate mix containing ATP, GTP, CTP and UTP was added to a final concentration of 100 μM (GTP, CTP and UTP) and 5 μM (ATP). Heparin (final 0.1 mg/ml) was simultaneously added to ensure single-round condition. After the time, 3.3 μCi [γ-^{32}P]ATP was added and the reaction was continued for 20 min. The reaction was then stopped by addition of phenol. In Figure 9, downstream-immobilized 169 bp template (atp major) was used to omit the addition of heparin. The amounts of RNA polymerase and immobilized DNA were 1.0 and 1.5 pmol, respectively, and [γ-^{32}P]GTP was used for labeling. The final concentrations of the NTPs were 100 μM (ATP, CTP UTP) and 5 μM (GTP).

Electrophoretic mobility shift assay

25 nM of RNA polymerase and 10 nM of labeled DNA template were incubated at 37 °C for 10 min in the standard (50 mM Tris-HCl, pH 7.9, 10 mM $MgCl_2$, 0.1 M KCl) or low (20 mM Tris-HCl, pH 7.9, 7 mM $MgCl_2$) salt conditions. 13% glycerol and 0.15 mg/ml Casein were also contained in the mixture. If necessary, transcription was started by adding the substrate mixture containing 5 μM ATP, 100 μM GTP, CTP, UTP, 0.1 mg/ml Heparin and incubated for 20 min. Some of the samples were treated with 3.5 units of *Hae*III for further 30 min before electrophoresis in a 5% polyacrylamide gel in TBE buffer. The gel was dried and subjected to autoradiography.

Exonuclease III footprinting

35 nM RNA polymerase was preincubated at 37 °C with 12 nM ^{32}P-labeled T7A1 DNA for 10 min in standard or low salt buffer, and then 40 μg/ml heparin was added to trap free enzyme originated from non-specific complex. Nucleotide mix (5 μM ATP, 100 μM GTP, CTP and UTP) was added 15 sec later, if necessary, and incubated for further 20 min, then the mixture was treated with 100 units of Exonuclease III (Toyobo) for 5 min. The reaction was stopped by phenol. DNA was precipitated with ethanol and loaded onto an 8% sequencing gel.

Fe^{2+}-induced site-specific radical cleavage

1.2 pmol of immobilized DNA template harboring the T7A1 or λP_RAL promoter and 1.0 pmol of RNA polymerase were incubated at 37 °C for 10 min in standard or low salt condition (for T7A1) or in standard or standard +100 mM NaCl (for λP_RAL). The immobilized binary complex was washed with buffer lacking $MgCl_2$. Then 0.1 mM $Fe(NH_4)_2(SO_4)_2$ was added and the mixture was incubated for a further 30 min. Cleavage was terminated by the addition of phenol and the reaction mixture was analyzed in an 8% sequencing gel.

Phenotypic analysis

Each strain was cultured in LB medium at 37 °C for overnight and then the culture is diluted with 0.84% NaCl. 2 μL of the diluted culture was spotted onto agar plates and incubated for 24 hours.

Preparation of total RNA

E.coli cells were cultured in LB medium until OD_{600} = 0.5 and then immediately chilled by adding pieces of ice into the culture. After centrifugation of it, the pelleted cells were suspended in buffer A (20 mM sodium acetate (pH 5.5), 10 mM EDTA) + 0.5% SDS. Then, the suspension was gently mixed with buffer A-satulated phenol (pH5.5) and heated at 60 °C for 5 min. Total RNA in water layer was precipitated with ethanol three times. Concentration of the final solution was determined by UV spectrometer (JASCO) as OD_{260}.

Northern hybridization

10 μg of total RNA was mixed in a loading buffer containing 1x MOPS running buffer (40 mM MOPS (pH 7.0), 10 mM Sodium acetate, 1 mM EDTA), 50% Formamide, 7.4% Formaldehyde, 8% Glycerol and 0.05 mg/ml Ethydium bromide, and heated at 60 °C for 10 min. The heat-treated sample was loaded onto a 1% agarose gel containing 1x MOPS running buffer and 1.3% formaldehyde. Electrophoresis was performed in 1x MOPS running buffer. RNAs in the gel were transferred onto a nylon membrane (Hynond N+, Amersham Pharmacia Biotech) by

capillary blotting method. The membrane was then treated with 50 mM NaOH for 5 min to immobilize RNA on it. Hybridization was carried out for more than 12 hours in a bottle with hybridization solution containing 5x SSC, 5x Denhardt's solution, 0.5% SDS, 17.5 μg/ml salmon sperm DNA and 1/2500 vol. of radio-labeled oligo DNA (20-mer). The hybridized membrane was washed twice in buffer 1 (2x SSC, 0.1% SDS), and then buffer 2 (0.1x SSC, 0.1% SDS). Nucleotide sequence of the Oligo DNAs was designed to hybridize a region corresponds to C-terminal end of the objective ORF. The sequence of the oligo DNAs (uncC(atpC)-N1, cspA-N1 and rpsA-N1) used for hybridization is summarized in Table 1.

In vitro transcription assay

In Figure 7B, 1.0 pmol of RNA polymerase and 1.5 pmol DNA were pre-incubated for 10 min at 37 °C in 8 μl of T-buffer (50 mM Tris-HCl (pH7.9), 100 mM KCl, 10 mM $MgCl_2$, 1 mM DTT, 150 μg/ml partially hydrolyzed casein). Transcription was started by adding substrates (20 μM [α-^{32}P]UTP, 0.5 mM ATP, GTP and CTP). After 20-min incubation at 37 °C, the reaction was quenched by addition of phenol. The synthesized RNA was loaded onto a 20% sequencing gel. In Figure 7C, 1.0 pmol of RNA polymerase and 0.5 pmol of DNA were used and NTPs (for *atp*, *rpsA* (P1) and *rpsA* (P3), 20 μM [γ-^{32}P]GTP, 0.5 mM ATP, CTP, UTP; for *cspA*, 20 μM [γ-^{32}P]ATP, 0.5 mM GTP, CTP, UTP) were added for transcription.

Primer extension

10 μg of total RNA was incubated at 60 °C for 10 min with 5'-^{32}P-labeled DNA in a reaction buffer containing 50 mM Tris-HCl (pH8.3), 100 mM KCl, 4 mM DTT and 10 mM $MgCl_2$. After denaturation, the mixture was placed at room temperature for 1.5 hours. Extension reaction was performed by adding dNTP mix (final 250 μM each) and 7.5-20 units of AMV reverse transcriptase XL (Takara), followed by incubation at 42 °C for 30 min. Synthesized cDNA was precipitated with ethanol and then loaded onto an 8% sequencing gel.

Table 1. Sequence of oligo DNAs used in this study.

Name	Sequence (5' -> 3')
PBRBAM1	CATGGCGACCACACCCGTCC
PBRBAM2	CGGCCACGATGCGTCCGGCG
T7Alds_L	AAGCGCTCATGAGCCCGAAG
delPRM1	CATACGTTACATCCCTCACCGCAAGGGATAAATAT
PRIMER1	GGCGTAGAGGATCTGCGCCC
atpIp_us	GGGTTAGCAGAAAAGTCGCAATTGTATGCA
atpIp-ds	AGGTATGCCGCGTGTCGTAT
cspA_F2	CGGCATTAAGTAAGCAGTTG
cspA_R3	CGAGGGGTATCAACGATAAC
rpsAp1_us1	ATTCCCACGCGTTCGTGAAGCATTATTGCG
rpsAp1_ds1	AACCAGTGGCGCTACCGCTCGGTTACGATC
rpsAp3_us1	TTTTGGCCGAGATCAAAGAACGCGACGACC
rpsAp3_ds1	TTGCAACGGGGGTACTGCAAATTCGGTCGC
metY-R1	TTATGAGCCCGACGAGCTAC
atpC-N1	TCGCTTTTTTGGTCAACTCG
cspA-N1	TACAGGCTGGTTACGTTACC
rpsA-N1	ACTCGCCTTTAGCTGCTTTG

Table 2. *E.coli* strains and plasmids used in the study.

	Genotype or properties	Reference or source
E.coli strains		
MC1061	F- *araD139 Δ(ara-leu)7696 galE15 galK16 Δ(lac)X74 rpsL*(Str^r) *hsdR2*($r_k^-m_k^+$) *mcrA mcrB1*	(43)
TK1001	MC1061 but *zgj*-203::Tn10	This study
TK1021	MC1061 but *greA*::*kan greB*::*cat zgj*-203::Tn10	This study
Plasmids		
pBR322	contains Tet^R gene from pSC101, ori and *rop* gene from the pMB1 and Amp^R gene from Tn3.	(44)
pMS001	contains 1.9 kbp fragment of *greA* and 3.2 kbp fragment of *greB* in pBR322.	This study
pMS002	contains 1.9 kbp fragment of *greA* in pBR322.	This study
pTK003	contains 3.2 kbp fragment of *greB* in pBR322.	This study

Table 3. Combinations of primers and template for PCR amplification

Name	Length (bp)	Primers (Forword, Reverse)	Template
Template I	154	PBRBAM1, PBRBAM2	pAR1435 (ref. 45)
Template II	250	PBRBAM1, T7A1ds_L	pAR1435 (ref. 45)
λP_RAL	191	delPRM1, PRIMER1	pλPR1AL32 (ref. 5)
atp	169	atp1p_us, atp1p-ds	Kohara clone #560 (ref. 16)
cspA	224	cspA_F2, cspA_R3	pJJG02 (ref. 46)
rpsA(P1)	268	rpsAp1_us1, rpsAp1_ds1	Kohara clone #217 (ref. 16)
rpsA(P3)	197	rpsAp3_us1, rpsAp3_ds1	Kohara clone #217 (ref. 16)

References

1. McClure, W. R. (1985) *Ann. Rev. Biochem.* **54**, 171-204
2. Shimamoto, N., Wu, F.Y.-H., and Wu, C.-H. (1981) *Biochemistry* **20**, 4745-4755
3. Sen, R., Nagai, H., Hernandez, V. J., and Shimamoto, N. (1998) *J. Biol. Chem.* **273**, 9872-9877
4. Kubori, T., and Shimamoto, N. (1996) *J. Mol. Biol.* **256**, 449-457
5. Kubori, T., and Shimamoto, N. (1997) *Nucleic Acids Res.* **25**, 2640-2647
6. Sen, R., Nagai, H., and Shimamoto, N. (2001) *Genes Cells* **6**, 389-401
7. Sen, R., Nagai, H., and Shimamoto, N. (2000) *J. Biol. Chem.* **275**, 10899-10904
8. Tagami, H., and Aiba, H. (1998) *EMBO J.* **17**, 1759-1767
9. Sparkowski, J., and Das, A. (1990) *Nucleic Acids Res.* **18**, 6443
10. Borukhov, S., Polyakov, A., Nikiforov, V., and Goldfarb, A. (1992) *Proc. Natl. Acad. Sci. USA* **89**, 8899-8902
11. Borukhov, S., Sagitov, V., and Goldfarb, A. (1993) *Cell* **72**, 459-466
12. Orlova, M., Newlands, J., Das, A., Goldfarb, A., and Borukhov, S. (1995) *Proc. Natl. Acad. Sci. USA* **92**, 4596-4600
13. Feng, G.-H., Lee, D. N., Wang, D., Chan, C. L., and Landick, R. (1994) *J. Biol. Chem.* **269**, 22282-22294
14. Hsu, L. M., Vo, N. V., and Chamberlin, M. J., (1995) *Proc. Natl. Acad. Sci. USA* **92**, 11588-11592
15. Zaychikov, E., Martin, E., Denissova, L., Kozlov, M., Markovtsov, V., Kashlev, M., Heumann, H., Nikiforov, V., Goldfarb, A., and Mustaev, A. (1996) *Science* **273**, 107-109
16. Kohara, Y., Akiyama, K., and Isono, K. (1987) *Cell* **50**, 495-808
17. Nielsen, J., Jorgensen, B. B., von Meyenburg, K., and Hansen, F. G. (1984) *Mol. Gen. Genet.* **193**, 64-71
18. Porter, A. C. G., Brusilow, W. S. A., and Simoni, R. D. (1983) *J. Bacteriol.* **155**, 1271-1278
19. Pedersen, S., Skouv, J., Kajitani, M., and Ishihama, A. (1984) *Mol. Gen. Genet.* **196**, 135-140
20. Tanabe, H., Goldstein, J., Yang, M., and Inoue, M. (1992) *J. Bacteriol.* **174**, 3867-3873
21. Jones, H. M., Brajkovich, C. M., and Gunsalus, R. P. (1983) *J. Bacteriol.* **155**, 1279-1287
22. Stahl, S. J., and Chamberlin, M. J. (1977) *J. Mol. Biol.* **112**, 577-601
23. Nierman, W. C., and Chamberlin, M. J. (1979) *J. Biol. Chem.* **254**, 7921-7926
24. Kammerer, W., Deuschle, U., Gentz, R., and Bujard, H. (1986) *EMBO J.* **5**, 2995-3000
25. Smagowicz, W. J., and Scheit, K. H. (1978) *Nucleic Acids Res.* **5**, 1919-1932
26. Oen, H., Wu, C.-W., Haas, R., and Cole, P. E. (1979) *Biochemistry* **18**, 4148-4155

27. Krummel, B., and Chamberlin, M. J. (1989) *Biochemistry* **28**, 7829-7842

28. Schickor, P., Metzger, W., Werel, W., Lederer, H., and Heumann, H. (1990) *EMBO J.* **9**, 2215-2220

29. Metzger, W., Schickor, P., Werel, W., Lederer, H., and Heumann, H. (1989) *EMBO J.* **8**, 2745-2754

30. Arndt, K. M., and Chamberlin, M. J. (1990) *J. Biol. Chem.* **213**, 79-108

31. Metzger, W., Schickor, P., Meier, T., Werel, W., and Heumann, H. (1993) *J. Mol. Biol.* **232**, 35-49

32. Altmann, C. R., Solow-Cordero, D. E., and Chamberlin, M. J. (1994) *Proc. Natl. Acad. Sci. USA* **91**, 3784-3788

33. Susa, M., Sen, R., and Shimamoto, N. (2002) *J. Biol. Chem.* in press.

34. Hernandez, V. J., Hsu, L. M., and Cashel, M. (1996) *J. Biol. Chem.* **271**, 18775-18779

35. Nagai, H., and Shimamoto, N. (1997) *Genes Cells* **2**, 725-734

36. Zhou, Y. N., Walter, W. A., and Gross, C. A. (1992) *J. Bacteriol.* **174**, 5005-5012

37. Owens, J. T., Chmura, A. J., Murakami, K., Fujita, N., Ishihama, A., and Meares, C. F. (1998) *Biochemistry* **37**, 7670-7675

38. Chan, C. L., and Gross, C. A. (2001) *J. Biol. Chem.* **276**, 38201-38209

39. McCarthy, J. E. G. (1990) *Mol. Microbiol.* **4**, 1233-1240

40. Kasimoglu, E., Park, S.-J., Malek, J., Tseng, C. P., and Gunsalus, R. P. (1996) *J. Bacteriol.* **178**, 5563-5567

41. Hernandez, V. J., and Cashel, M. (1995) *J. Mol. Biol.* **252**, 536-549

42. Chapon, C. (1982) *J. bacteriol.* **150**, 722-729

43. Wertman, K. F., Wyman, A. R., and Botstein, D. (1986) *Gene* **49**, 253-262

44. Watson, N. (1988) *Gene* **70**, 399-403

45. Dunn, J. J., and Studier, F. W. (1983) *J. Biol. Chem.* **166**, 477-535

46. Goldstein, J., Pollitt, N. S., and Inouye, M. (1990) *Proc. Natl. Acad. Sci. USA* **87**, 283-287

47. Fujioka, M., Hirata, T., and Shimamoto, N. (1991) *Biochemistry* **30**, 1801-1807.

Acknowledgments

First of all, I am grateful to Dr. Nobuo Shimamoto for suggesting the main themes of my thesis, teaching some techniques, discussions and advices. Dr. Hiroki Nagai, Dr. Tomoko Kubori and Dr. Ranjan Sen gave me a lot of materials, strains and data that help me for proceeding my work. I thank Dr. Kumiko Sogawa and laboratory members for their advices. I am grateful to Prof. Akira Ishihama for critical advice extracted from his numerous knowledge of transcription. I thank Prof. Makio Tokunaga, Prof. Hiroyuki Araki and Ass. Prof. Yasuo Shirakihara for critical comments on my progress reports. I also thank Prof. Hiroji Aiba for discussion. Dr. Tatsuhiko Abo and Koji Ueda kindly taught me a Northern hybridization technique. Emi Horiuchi helped me with her secretaryship. I thank the ITOH scholarship foundation for financial support in my graduate school days. Finally, I am grateful to Yokonomi-kai members who always encourage me.